Optimal Combination Approach for Frequency Regulation in Restructured Power Grid Utility

S. Jennathu Beevi and R. Jayashree
B.S. Abdur Rahman Crescent Institute of Science and Technology, Chennai, India
Email: jennathb@gmail.com; jayashree@crescent.education

***Abstract*—This paper aims to design an optimal controller in order to regulate the frequency in restructured power grid utility. Integral (I), Proportional-Integral (PI) and Proportional Integral Derivative (PID) controllers have been employed for frequency control. A two-area power system in a restructured environment is studied for the proposed approach. Gain tuning of the controllers is achieved through Ant Lion Optimization (ALO) algorithm by employing three objective functions, namely, Integral Absolute Error (IAE), Integral Squared Error (ISE) and Integral Time Absolute Error (ITAE). The objective functions are tested with I, PI and PID controllers for two cases, namely, bilateral contracts with and without violation respectively. Comparison of different combinations is done in terms of the performance indices. PID-ITAE combination gives acceptable results. An optimal combination approach is effective for finding the best combination of controller and objective function which helps to achieve improved steady-state performance.**

***Index Terms*—Automatic generation control, control engineering, heuristic algorithms, optimization, power system control**

I. Introduction

Deregulated market structure, based on Electricity Act 2003, administers the electricity power producers to compete among them and sell power to the consumers directly. Currently, in Indian grid, the frequency band permissible under normal operating conditions is 49.90 Hz to 50.05 Hz which could be further stiffened to 49.95 Hz to 50.05 Hz by 2020, as per the report by Central Electricity Regulatory Commission (CERC), November 2017. In order to regulate the frequency and maintain its value within the permissible band, additional active power generation must be fed into the power grid to balance the excess load. The real-time power system is a composition of different areas with multiple Generation Companies (GCs) which are interconnected for power exchange with the transmission lines. These transmission lines are referred to as tie lines. Any variation in load demand from a particular area Distribution Company (DC) can be regulated by feeding in active power through a GC in an interconnected area, to maintain a constant frequency. The control in the generation is done through Automatic Generation Control (AGC) which is also termed as 'frequency regulation' in the restructured environment. AGC is one of the ancillary services in the restructured power system.

AGC in restructured power system has been discussed [1]-[7] by several authors over the years. The classical Integral (I), Proportional Integral (PI) and Proportional Integral Derivative (PID) controllers have been used by several researchers in the past for frequency control in conventional Vertically Integrated Utility (VIU) structure as well as restructured power systems. Dash *et al*. [8] discussed automatic generation control for unequal three areas with generation rate constraint and implemented I, PI and PID controllers. Khodabakhshian *et al*. [9] introduced a new robust PID controller whose specifications depend on maximum overshoot level, which was implemented for AGC of hydro systems. Artificial neural network [10] and fuzzy logic [11] based controllers have been implemented for AGC. There has been growing interest in nature-inspired heuristic algorithms, in recent times, which has motivated for solving many problems in the areas of automation, robotics, power systems, etc. in an efficient manner. The controller gains are tuned using several nature-inspired algorithms. Abraham *et al*. [12] applied a genetic PID control for frequency control in a hydrothermal system. Satheeshkumar *et al*. [13] Applied ant Lion Optimization (ALO) algorithm for three area interconnected system with PI controller and compared its gain and other performance parameters with Genetic Algorithm (GA), BAT optimization algorithm, and Particle Swarm Optimization (PSO) algorithms. Saikia *et al.* [14] evaluated the robustness in unequal three area system with different controllers I, PI, PID, PID plus Double Derivative (DD), optimizing them using ALO algorithm and compared with conventional PID controller. The authors in [15] have implemented optimized PI-Proportional Derivative (PD) cascade controllers for multi-area AGC. PID plus second order derivative controller optimized by ALO has been applied by the authors in [16]. In recent years, several intelligence control techniques and optimization algorithms [17]-[23] were applied for frequency control in restructured power systems. In optimization by these algorithms, objective function plays a major role in all these works of literature listed above, the reason for selecting a suitable controller

Manuscript received May 19, 2019; revised June 28, 2019; accepted July 20, 2019.

Corresponding author: S. Jennathu Beevi (email: jennathb@ gmail.com).

doi: 10.18178/ijeetc.9.1.28-37

and an objective function has not been justified. The controller is selected based on the general performance characteristics of I, PI and PID controllers and optimized using Integral Absolute Error (IAE), Integral Squared Error (ISE) and Integral Time Absolute Error (ITAE) as objective functions. A proper numerical quantitative analysis has not been given by the authors to select a particular objective function. Therefore, in our present work, we aim to achieve the following objectives so as to arrive at an optimal controller-objective function combination through qualitative and quantitative analysis.

Our present work has been split into three phases.

- Tuning of the I, PI and PID controller gains by optimizing the objective functions Integral Absolute Error (IAE), Integral squared error (ISE).
- Integral Time Absolute Error (ITAE) for bilateral contract and contract violation scenario.
- Analysis to find the optimal combination of controller and objective function.
- Analysis of the robustness of the identified optimal combination for bilateral contracts for 10%, 20% and 30 % increase in load.

ALO has been used for solving many unconstrained and constrained problems. ALO is found effective in many engineering applications due to its good convergence speed and its ability to find solutions in unknown search spaces. Hence, ALO algorithm has been used for tuning the controller gains in our present work.

II. System under Study

In the proposed model, the interconnected two identical area power system consists of two non-reheat thermal units. Various entities involved in a restructured environment are gencos (GC), transmission companies (TRANSCO) and discos (DC). GC is an owner-operator of one or more generators and bids the power into the competitive marketplace.

DC is the monopoly franchise owner-operator of the local power delivery system, which delivers power to individual businesses and homeowners. In the restructured power system, there are two types of frequency related services, one is the frequency regulation which accounts for changes in load from minute to minute land, and the other type is load following which takes care of the load for a longer duration. In our present work, the frequency regulation alone is considered for simulation analysis without and with contract violation.

The transfer function model of the system considered is shown in Fig. 1.

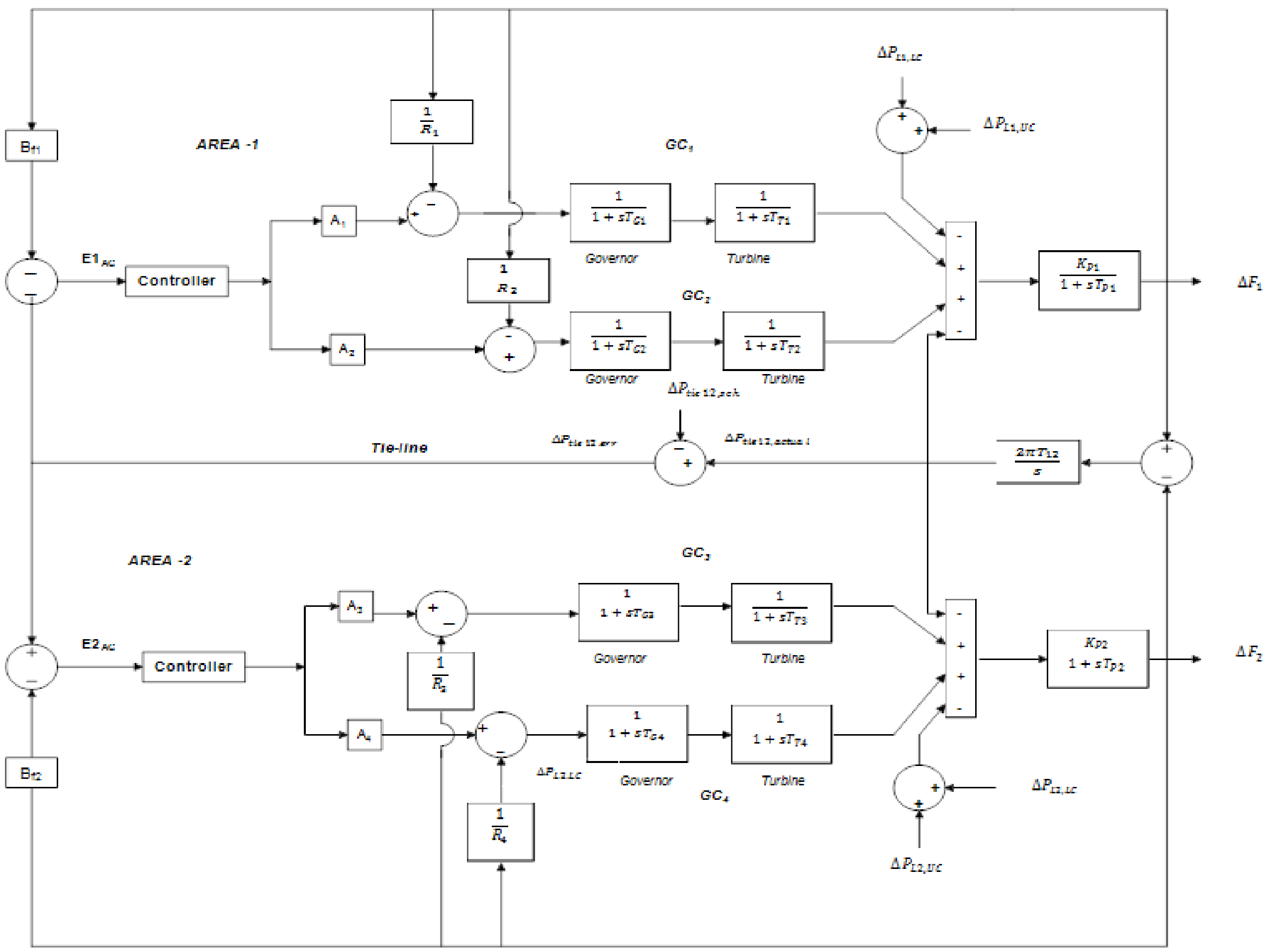

Fig. 1. Two area system for AGC in the restructured power market.

The dynamics of governor, turbine and power system are represented by their respective transfer functions, $G_g(s)$, $G_t(s)$ and $G_p(s)$.

Area control error of (E_{AC}) of the two areas are given by

$$E1_{AC} = B_{f1}\Delta F_1 + \Delta P_{\text{tie12,err}} \quad (1)$$

$$E2_{AC} = B_{f2}\Delta F_2 + \alpha_{12}\Delta P_{\text{tie21,err}} \quad (2)$$

where B_{f1} and B_{f2} are the frequency bias factors in Area-1 and Area-2 respectively. ΔF_1 and ΔF_2 are the frequency deviations of Area-1 and Area-2 respectively, and $\alpha_{12} = -P_{r1}/P_{r2}$, P1 and P2 are the rated capacities of Area-1 and Area-2 respectively.

TABLE I. NOMENCLATURE

K_P	Gain of the power system
T_P	Time constant of the power system
T_t	Time constant of the Turbine
T_g	Time constant of the Governor
T_{12}	Time constant of the tie line
R	Speed regulation due to governor action
ΔF	Frequency deviation
ΔP_{tie12}	Power exchange in between area 1 and 2 via tie-line
$\Delta P_{L1,\,UC}$	Noncontracted load demand
A_1, A_2	E_{AC} of GCs 1 & 2 in Area-1
A_3, A_4	E_{AC} of GCs 3 &4 in area-2

TABLE II. TRANSFER FUNCTION AND THE NOMINAL PARAMETERS OF THE POWER SYSTEM

Component	Transfer function	Nominal values
Governor	$G_g(s) = 1/(1+sT_{gi})$	$T_{g1} = T_{g2}$ =0.08 s
Turbine	$G_t(s) = 1/(1+sT_{ti})$	$T_{t1} = T_{t2}$ =0.3 s
Power system	$G_p(s) = K_{pi}/(1+sT_{pi})$	$K_{p1} = K_{p2}$ = 120 $T_{p1} = T_{p2}$ = 20 s
Governor droop	$1/R_i$	$R_1 = R_2$=2.4Hz/pu.MW
Bias	B_{fi}	$B_{f1} = B_{f2}$ = 0.4249
Tie-line	$2\Pi T_{12}/s$	0.543848 /s

The symbols used in the block diagram are explained in Table I.

$\Delta P_{\text{tie12,err}}$ is represented by

$$\Delta P_{\text{tie12}(s)} = \frac{2\pi T_{12}}{s} \quad (3)$$

The transfer function of the components in the two-area power system and the nominal values of the parameters used are given in Table II.

In the proposed system, there are two control areas in which each area has two GCs and two DCs respectively. Both the GCs have non-reheat thermal units and the DCs have the freedom to contract with any GC. Any DC in Area-1 may contract with any GC in another control area, say Area-2, independently through a bilateral transaction. The Independent System Operator (ISO) approves the feasible transactions and also has the responsibility of ensuring the reliability and security of the entire system. DC Participation Matrix (DPM) demonstrates the various contracts that exist between GCs and DCs expressed by contract participation factors (fcp). The diagonal blocks of the DPM given by (4) corresponds to local demands i.e., the demands of DCs in an area from the GCs in the same area. The demand of the DCs in one area from the GCs in another area is represented by the off-diagonal blocks.

$$\text{DPM} = \begin{bmatrix} \text{fcp}_{11} & \text{fcp}_{12} & \text{fcp}_{13} & \text{fcp}_{14} \\ \text{fcp}_{21} & \text{fcp}_{22} & \text{fcp}_{23} & \text{fcp}_{24} \\ \text{fcp}_{31} & \text{fcp}_{32} & \text{fcp}_{33} & \text{fcp}_{34} \\ \text{fcp}_{41} & \text{fcp}_{42} & \text{fcp}_{43} & \text{fcp}_{44} \end{bmatrix} \quad (4)$$

The summation of column entries in DPM matrix is unity, i.e.

$$\sum_{i=1}^{4} \text{fcp}_{ij} = 1; \text{ for } j = 1,\ 2,\ 3,\ 4 \quad (5)$$

where i and j are the subscripts used to denote GC and DC respectively.

The power contracted by DCs with GCs is given as

$$\Delta P_{gci} = \sum_{j=1}^{4} \text{fcp}_{ij}\Delta P_{Lj} \quad \text{for } i = 1,\ 2,\ 3,\ 4 \quad (6)$$

where ΔP_{gci} is the contracted power of ith GC, ΔP_{Lj} is the total demand of DC_j and fcp_{ij} is the contract participation factor between jth DC and ith GC.

The power flow scheduled on the tie-line at steady state is given as

$$\Delta P_{gci} = \sum_{j=1}^{4} \text{fcp}_{ij}\Delta P_{Lj}; \text{ for } i = 1,\ 2,\ 3,\ 4 \quad (7)$$

The steady state power flow scheduled, in the tie-line for the bilateral contracts in terms of fcp is given as

$$\Delta P_{\text{tie12,shd}} = \sum_{i=1}^{2}\sum_{j=3}^{4} \text{fcp}_{ij}\Delta P_{Lj} - \sum_{i=3}^{4}\sum_{j=1}^{2} \text{fcp}_{ij}\Delta P_{Lj} \quad (8)$$

The error in tie-line power flow is defined as

$$\Delta P_{\text{tie12,err}} = \Delta P_{\text{tie12,actual}} - \Delta P_{\text{tie12,shd}} \quad (9)$$

At steady state, the error in tie-line power flow, $\Delta P_{\text{tie12,err}}$ becomes zero as the actual tie-line power flow is equal to the power flow scheduled. This error signal is used to generate the respective E_{AC} signals as in the traditional scenario. The change in load demand by a DC is represented as a local load in the area the DC belongs. This corresponds to the local loads $\Delta P_{L1,LC}$ in Area-1 and $\Delta P_{L2,LC}$ in Area-2 where $\Delta P_{L1,LC} = \Delta P_{L1} + \Delta P_{L2}$ and $\Delta P_{L2,LC} = \Delta P_{L3} + \Delta P_{L4}$. ΔP_{L1} , ΔP_{L2} , ΔP_{L3} , and ΔP_{L4} are the contracted power demanded by the four DCs, DC_1, DC2, DC_3, and DC_4 respectively from the various GCs. ΔP_{UC1} , ΔP_{UC2} , ΔP_{UC3} , and ΔP_{UC4} are the noncontracted demands of the four DCs respectively. When there is a scenario that a DC claims more power than that specified in the contract and violates the contract, this additional power should be supplied by the GC in the same area as that of DC that violates the contract. In each area, the ACE participation factors (apfs) decide the distribution of noncontracted steady state power among various GCs. It should be noted that the apfs, A_1+A_2=1.0 in Area -1 and A_3+A_4=1.0 in Area-2.

III. Case Description

A. Case 1: Bilateral Contracts without Contract Violation

In this case, an arrangement is made between GCs and DCs by which each party (GC or a DC) promises to perform an act in exchange for the other party's act. The DCs in Area-1 and Area-2 can contract with GCs in Area-1 and Area-2 for exchange of power. The contracts can be understood with the help of DPM matrix. It is assumed that each DC demands 0.05 p.u. MW power from GCs as defined by fcps in DPM matrix.

$$\text{DPM} = \begin{bmatrix} 0 & 0.3 & 0.25 & 0.2 \\ 0.6 & 0.2 & 0 & 0.2 \\ 0.2 & 0.4 & 0.25 & 0.6 \\ 0.2 & 0.1 & 0.50 & 0 \end{bmatrix} \tag{10}$$

Thus

$$\Delta P_{L1} = \Delta P_{L2} = \Delta P_{L3} = \Delta P_{L4} = 0.05 \text{ p.u. MW}.$$

$$\Delta P_{L1,LC} = \Delta P_{L1} + \Delta P_{L2} = 0.1 \text{ p.u. MW}$$

$$\Delta P_{L2,LC} = \Delta P_{L3} + \Delta P_{L4} = 0.1 \text{ p.u. MW}.$$

Since there are no noncontracted power demands in either of the areas, $\Delta P_{L1,UC} = \Delta P_{L2,UC} = 0.0$ p.u. MW. Each GC participate in AGC is defined by the following apfs: A_1 is 0.6, A_2 is 0.4, A_3 is 0.7 and A_4 is 0.3. According to (8), the scheduled tie-line power flow is calculated as 0.0125 p.u. MW. At steady state, the generation of a GC must match the demand of the DC which is in contract with it.

B. Case 2-Bilateral Contracts with a Contract Violation

In this case, a DC in a particular area may violate a contract by demanding more than that specified in the contract. This excess power is not contracted out to any GC and must be supplied by the GCs in the same area as that of the DC. Therefore, it must be reflected as a noncontracted local load of that area. Let only DC_1 of Area-1 demands 0.05 p.u.MW of excess power. i.e., $\Delta P_{UC1} = 0.05$ p.u. MW and DC_2 of Area-2 demands no excess power, i.e., $\Delta P_2 = 0$ p.u.MW. Therefore, the total noncontracted load in Area-1, $\Delta P_{L1,UC} = \Delta P_{UC1} + \Delta P_{UC2}$ =0.05+0=0.05 p.u. MW. Similarly, $\Delta P_{UC3} = 0.05$ p.u. MW; $\Delta P_{UC4} = 0$ and hence, $\Delta P_{L2,UC} = \Delta P_{UC3} + \Delta P_{UC4}$ =0.05 p.u. MW. Considering the same DPM and same E_{AC} participation factors (apfs) and that each DC has a contracted power of 0.05 p.u. MW**.** We have $\Delta P_{L1,LC}$ $= \Delta P_{L1} + \Delta P_{L2} = (0.05 + 0.05) = 0.1$ p.u. MW (contracted load) and $\Delta P_{L2,LC} = \Delta P_{L3} + \Delta P_{L4} = (0.05 + 0.05) = 0.1$ p.u. MW (contracted load).

$$\begin{bmatrix} \Delta P_{g1,ss} \\ \Delta P_{g2,ss} \\ \Delta P_{g3,ss} \\ \Delta P_{g4,ss} \end{bmatrix} = \begin{bmatrix} \text{fcp}_{11} & \text{fcp}_{12} & \text{fcp}_{13} & \text{fcp}_{14} \\ \text{fcp}_{21} & \text{fcp}_{22} & \text{fcp}_{23} & \text{fcp}_{24} \\ \text{fcp}_{31} & \text{fcp}_{32} & \text{fcp}_{33} & \text{fcp}_{34} \\ \text{fcp}_{41} & \text{fcp}_{42} & \text{fcp}_{43} & \text{fcp}_{44} \end{bmatrix} \begin{bmatrix} \Delta P_{L1} \\ \Delta P_{L2} \\ \Delta P_{L3} \\ \Delta P_{L4} \end{bmatrix} + \begin{bmatrix} A_1 & 0.0 & 0.0 & 0.0 \\ 0.0 & A_2 & 0.0 & 0.0 \\ 0.0 & 0.0 & A_3 & 0.0 \\ 0.0 & f\,0.0 & 0.0 & A_4 \end{bmatrix} \tag{11}$$

It is assumed that the noncontracted power is demanded by DC_1 in Area-1. GC_1 and GC_2 are also in Area-1. Therefore, at steady state, this noncontracted power demand must be generated by GC_1 and GC_2 of Area-1 in proportion to their E_{AC} participation factors plus they will also generate their contracted power demand. Hence, using (6) the steady state outputs of the GCs in Area- 1 and Area- 2 are calculated. The scheduled tie-line power is calculated as 0.0125 p.u. MW. The steady-state outputs of the GCs in Area -1 and Area-2 are calculated for Case 1 and Case 2 and given in Table III.

TABLE III. STEADY STATE OUTPUTS OF GC_S IN AREA-1 AND AREA-2

GCs	Case 1	Case 2
$\Delta P_{g1,ss}$	0.0375	0.0675
$\Delta P_{g2,ss}$	0.05	0.07
$\Delta P_{g3,ss}$	0.0725	0.1075
$\Delta P_{g4,ss}$	0.04	0.055

IV. Objective Function and Control Strategy

PID abbreviated as a proportional integral derivative controller popularly used in industrial systems due to their control feedback technique. Error calculation depends on the deviation from the desired value to the measured value. This deviation is reduced by manipulation of the variables which responds to the controller. The controller transfer function is given as follows:

$$C(s) = K_P + \frac{K_I}{s} + K_D s \tag{12}$$

where K_P is the proportional gain, K_I is the integral gain and K_D is the derivative gain.

The controller parameters (K_P, K_I, K_D) are tuned using ALO Algorithm. The main requirement for the objective function under AGC is to minimize the frequency error deviation and tie line power deviations within a short span of time. IAE integrates the absolute error over time. It does not add weight to any of the errors in a system's response. ISE integrates the square of the error over time. ISE will penalize large errors more than smaller ones. ITAE criteria give integration of time multiplied by absolute error and the weight is given to those which exists over a longer time than those at the initial stage. The reduction in settling time is achieved by allocating larger multiplication factor to the error at final stages rather than the initial ones. The three objective functions considered for optimization are given as,

$$J_1 = IAE = \int_0^t |\Delta F_1| + |\Delta F_2| + |\Delta P_{tie}| dt \,. \quad (13)$$

$$J_2 = ISE = \int_0^t (\Delta F_1^2 + \Delta F_2^2 + \Delta P_{tie}^2) dt \,. \quad (14)$$

$$J_3 = ITAE = \int_0^t |\Delta F_1| + |\Delta F_2| + |\Delta P_{tie}|.t.dt \,. \quad (15)$$

where ΔF_1 and ΔF_2 are the system frequency deviation in Area-1 and Area-2 respectively. ΔP_{tie} is the incremental change in tie-line power and t is the time interval of simulation. The constraints are the limits on controller gains. Therefore, the design problem can be formulated as the following optimization problem.

Minimize J_1, J_2 and J_3 subjected to

$$K_{IL} \le K_I \le K_{IU} \,. \quad (16a)$$

$$K_{PL} \le K_P \le K_{PU} \,. \quad (16b)$$

$$K_{DL} \le K_D \le K_{DU} \,. \quad (16c)$$

where J_1, J_2 and J_3 are the objective functions denoted in (13)-(15) and the lower and upper bounds for the controller gains are given in (16a-16c).

V. Ant Lion Algorithm [24]

The closed loop gain tuning of the controllers is carried out by minimum error criteria method by optimizing the three objective functions, as mentioned in Section 3. For optimization, the ALO algorithm has been applied. ALO is a search algorithm which imitates the hunting techniques of Ant Lion in nature. In this technique, ant lions and ants are considered as search agents to figure out the solution by following the procedure sets for hunting the prey. The sets involve the randomized walk of ants, trap building, entrapment of ants, catching prey and reconstructing the traps. The position of the ants is dependent on a random walk around the ant lion. The selection is made by roulette wheel and the elite selection. Elite setting in search process ensures the best particle is presented. Choice of ALO for automatic generation control is dependent on its good convergence, high efficiency, and faster calculation speed. The flowchart for the ALO algorithm is given in Fig. 2.

The optimal gains are obtained using the Ant lion optimization algorithm. For each case there are nine combinations available, hence comparing ALO with other algorithms will lead to many more combinations deviating from the scope of the paper. Also, ALO has good convergence speed which is compared with that of other algorithms like moth flame algorithm (MFO) and Whale Optimization Algorithm (WOA).

The time taken for convergence is given in Table IV. As seen from the table ALO takes less time to converge and give the results when compared to other algorithms.

TABLE IV. Comparison of Computational Time

Algorithm	Computational time (s)
ALO	4451.124637
MFO	5737.004527
WOA	6294.284866

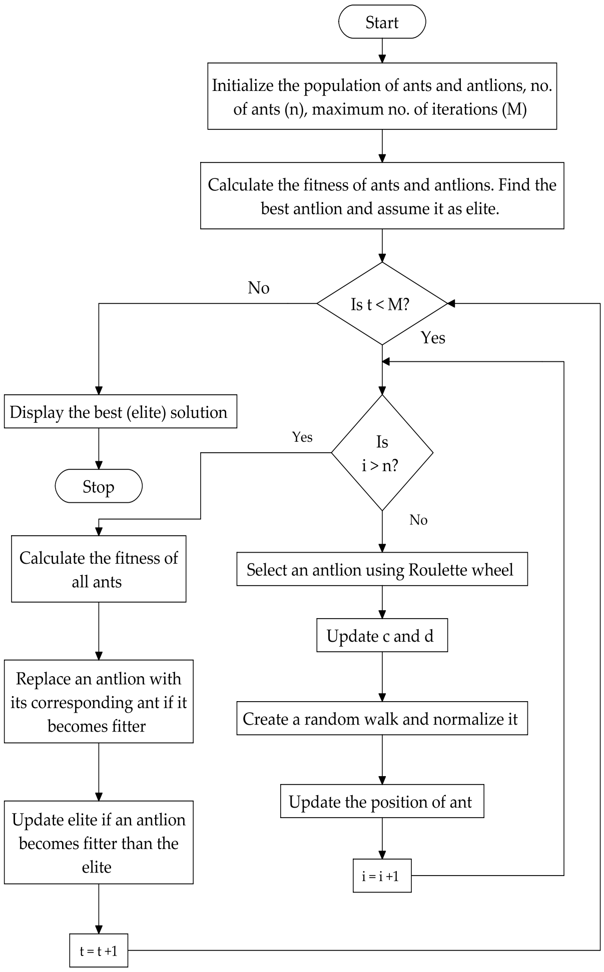

Fig. 2. Flowchart for Ant lion optimization algorithm.

Ants in nature move in complex patterns in search of food. These complex patterns are termed as randomized walk and are modeled as follows:

$$X(t) = \begin{bmatrix} 0, \text{ cumsum}(2r(t_1)-1), \\ \text{cumsum}(2r(t_2)-1), \; \ldots \\ \text{cumsum}(2r(t_n)-1) \end{bmatrix} \quad (17)$$

where *cumsum* is to calculate cumulative sum, n is maximum number of iterations and $r(t)$ is stochastic function.

The stochastic function is defined as

$$r(t) = \begin{cases} 1, \text{ if rand} \ge 0.5 \\ 0, \text{ if rand} \le 0.5 \end{cases} \quad (18)$$

where *rand* is a random number with a uniform distribution within an interval.

The following equation describes randomized walk made inside a search space:

$$X_i^t = \frac{(X_i^t - a_i) \times (d_i^t - c_i^t)}{(b_i - a_i)} + C_i \quad (19)$$

where a_i and b_i are the minimum and maximum values of the randomized walk of ith variable, c_i^t and d_i^t are the minimum and maximum of ith variable in the tth iteration.

The results of location of ants are stored in the form of a matrix:

$$M_{\text{Ant}} = \begin{bmatrix} A_{1,1} & A_{1,2} & \cdots & \cdots & A_{1,d} \\ A_{1,1} & A_{1,2} & \cdots & \cdots & A_{1,d} \\ \cdots & \cdots & \cdots & \cdots & \cdots \\ \cdots & \cdots & \cdots & \cdots & \cdots \\ A_{n,1} & A_{n,2} & \cdots & \cdots & A_{n,d} \end{bmatrix} \tag{20}$$

where M_{Ant} is the matrix for saving the position of each ant, $A_{i,j}$ shows the value of the jth variable dimension of ith ant, n is the number of ants, d is the number of variables.

The objective value of each ant lion is evaluated and stored in the matrix given by

$$M_{\text{OA}} = \begin{bmatrix} f\left(|A_{1,1} \ \ A_{1,2} \ \cdots \ A_{1,d}|\right) \\ f\left(|A_{2,1} \ \ A_{2,2} \ \cdots \ A_{2,d}|\right) \\ \vdots \\ f\left(|A_{n,1} \ \ A_{n,2} \ \cdots \ A_{n,d}|\right) \end{bmatrix} \tag{21}$$

where M_{OA} matrix gives the fitness value of the location of ants in corresponding matrix M_{Ant}.

The operation of a roulette wheel is employed in trap building to select fitter Ant lions during the process of optimization. This process induces the fittest Ant lions to catch the ants, and there is an increase of probability of catching the ants. Entrapment can be explained mathematically by

$$c_i^t = \text{Ant lion}_j^t + c^t \tag{22}$$

$$d_i^t = \text{Ant lion}_j^t + d^t \tag{23}$$

where the Ant position for selected Ant lion is Ant lion_j^t . Ant lion shoots ant sand towards the position of the ant so that slide motion of the ant is initiated. The above process can be expressed using the equations

$$C^t = c^t / I \tag{24}$$

$$D^t = d^t / I \tag{25}$$

$$I = 10^{\omega}\, t/T \tag{26}$$

where t is the current iteration, T is maximum number of iterations. The process of catching the prey and reconstruction of pit takes place only when the fitter ant slides inside the sand than the respective ant lion. The updation of position is required for the Ant lion to the latest position to increase the chance of catching more preys.

The following equation shows this behavior.

$$\text{Ant lion}_j^t = \text{Ant}_j^t, \text{ if } f(\text{Ant}_j^t) > f(\text{Ant lion}_j^t) \tag{27}$$

Evolutionary algorithms have this trait called elitism which enhances the best solution to be maintained in an optimization process. In this case, the fittest ant lion in each iteration is stored and is taken as elite. The elite ant lion affects the movement of all ants during iterations carried. The selection of ant lion to which randomized walk of ants is carried out by roulette wheel and elite. The following equation describes this behavior:

$$\text{Ant}_j^t = \frac{R_A^t + R_E^t}{2} \tag{28}$$

where R^i_A is a randomized walk around ant lion selected by roulette wheel at tth iteration, R^t_E is the randomized walk around the elite at tth iteration, and Ant_j^t indicates the position of ith ant and tth iteration.

VI. Results and Discussion

A. Quantitative and Qualitative Analysis: Case 1

A series of simulations have been performed using Simulink in MATLAB to tune the controller parameters. The algorithm parameters are the number of agents and a maximum number of iterations. All the three objective functions are applied with I, PI and PID controllers to analyze the dynamic and steady-state performance of the power system. To implement the ALO algorithm, the number of search agents is set as 50 and the maximum number of iterations chosen as 100. The lower and upper bounds for the controller gains are –10 and 10 respectively. The best score obtained in the ALO optimization process with the performance indices IAE, ISE and ITAE with I, PI and PID controllers is depicted in Table V for Bilateral Contracts. In order to show the ability and efficiency of the proposed method, a comparison of performance indices is carried out for the PID, PI and I controllers.

TABLE V. Comparison of the Best Costs-Case 1

Criterion	Controller	Best cost
IAE	I	0.2484
	PI	0.2543
	PID	0.0435
ISE	I	0.0157
	PI	0.0139
	PID	0.0004
ITAE	I	0.4873
	PI	0.4701
	PID	0.0464

From Table V, it is observed that ISE with I, PI and PID is better than other combinations with respect to the best cost value. But, the dynamic performance of PI-ISE combination is found to be poor. ITAE-PID gives comparably reduced cost function and shows good transient and steady state performance. PID with IAE also gives a cost function of 0.0435 but it results in poor damping which can be observed from frequency response curves. The gains of the controllers optimized using ALO algorithm are given in Table VI for bilateral contracts without violation.

TABLE VI. Optimized Gains of the Controllers - Case 1

Controller		J_1	J_2	J_3
I	k_{i1}	-0.000071	-0.0051	0.2658
	k_{i2}	-0.0000353	-0.0048	0.1878
PI	k_{i1}	-0.0000409	-0.0170	0.2664
	k_{i2}	0.0000444	-0.0119	0.1759
	k_{p1}	0.1762	0.4002	-0.0734
	k_{p2}	0.0877	0.2593	-0.0829
PID	k_{p1}	5.7035	5.146	6.2869
	k_{p2}	4.9023	4.4318	1.1242
	k_{i1}	8.4679	5.848	6.5573
	k_{i2}	6.4552	9.970	1.3276
	k_{d1}	3.1330	3.277	2.1073
	k_{d2}	2.1112	2.2922	0.5332

The performance indices namely undershoot, overshoot and settling time obtained through simulation results are given in Table VII.

As seen from Table VII, ITAE-PID has given the least value for settling time for frequency deviations in Area-1 and Area-2 and tie-line power deviation. ISE-PI shows higher values of settling times. The improvement in settling time with ALO optimized PID-ITAE over PID-ISE and PID-IAE combination for ΔF_1 is found to be 67% and 50% respectively. The settling time for ΔF_2 has been improved with PID-ITAE by41 % and 10% respectively compared with that of PID-ISE and PID-IAE combinations. For the tie-line power deviation, the improvement in settling times with optimized PID -ITAE over PID-ISE and PID-IAE controllers are found to be 52% and 40% respectively. The overshoot, undershoot of deviations in frequencies and tie-line power exchange with PID controller are much reduced compared to those of PI and I controllers.

TABLE VII. PERFORMANCE INDICES-CASE 1

Criterion	Controller	ST(s)			US (Hz & puMW)			OS (Hz and puMW)		
		Δk_1	Δk_2	ΔP_{tie}	ΔF_1	ΔF_2	ΔP_{tie}	ΔF_1	ΔF_2	ΔP_{tie}
IAE	I	8	8	10	0.130	0.110	0.01	0.050	0.045	0.0120
	PI	12	14	11	0.120	0.110	0.011	0.050	0.060	0.0012
	PID	6	5.5	8	0.035	0.020	0.008	0.010	0.016	0.0120
ISE	I	9	10	9	0.130	0.110	0.012	0.050	0.050	0.0125
	PI	25	30	35	0.115	0.105	0.012	0.060	0.0687	0.0125
	PID	9	8.5	10	0.035	0.019	0.020	0.000	0.0163	0.0125
ITAE	I	11	14	16	0.130	0.150	0.013	0.081	0.0800	0.0030
	PI	9	11	14	0.130	0.120	0.001	0.080	0.0850	0.0125
	PID	**3**	**5**	**4.8**	0.039	0.041	0.012	0.0012	0.0075	0.0137

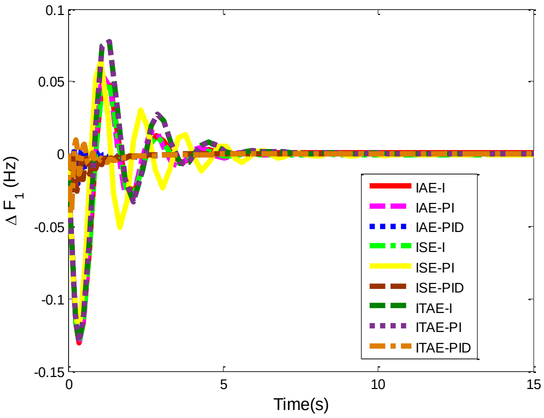

Fig. 3. Frequency deviation of Area-1- Case 1.

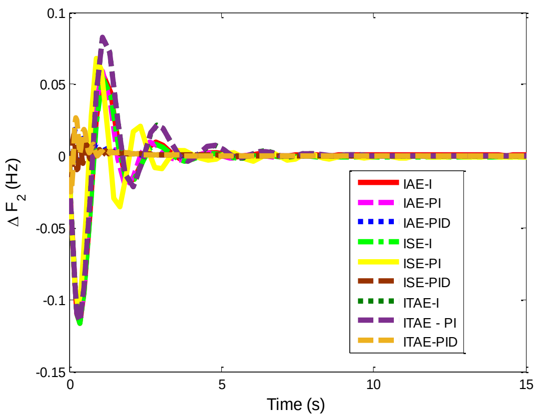

Fig. 4. Frequency deviation of Area-2- Case 1.

For Case1, with 10% load perturbation, (i.e.) 0.1puMW, Fig. 3 shows the frequency deviation in Area-1 and Fig. 4 shows the frequency deviation in Area-2. The tie-line power deviations for different controller-objective function combination are shown in Fig. 5. The generation responses of the GCs are shown in Fig. 6. With ITAE-PID, the frequency deviations and tie line power deviations of the thermal unit settles to a steady state at a faster rate and undershoot and overshoots are also reduced. The damping is also good. But the PI and I controllers optimized with ISE exhibit larger overshoot and undershoot values. The tie-line power deviations obtained by PI and I controllers are seen with fewer fluctuations whereas the PID have given a smooth curve without much fluctuations.

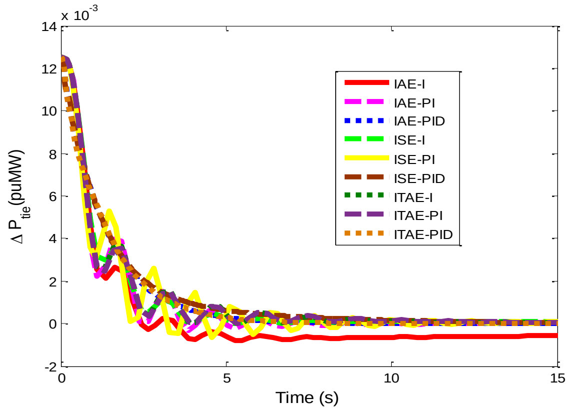

Fig. 5. Tie-line power deviation between Area1 and Area 2- Case 1.

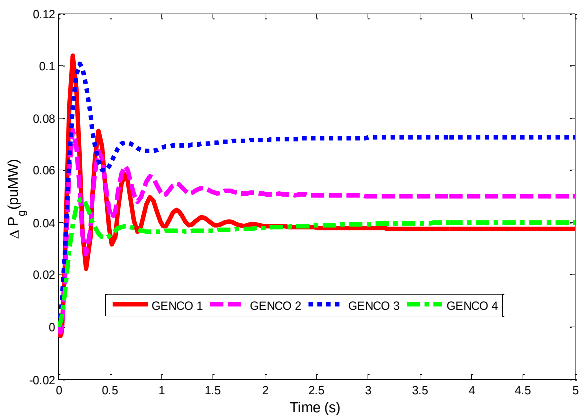

Fig. 6. Generation response of the GCs in Area-1&2- Case 1.

TABLE VIII. OPTIMIZED GAINS OF CONTROLLERS WITH ITAE - CASE 2

Controller	Best cost	Optimized Gains	
I	0.3696	k_{i1}	0.1490
		k_{i2}	0.1205
PI	0.3173	k_{i1}	0.1064
		k_{i2}	0.0833
		k_{p1}	-0.1939
		k_{p2}	-0.1589
PID	0.01150	k_{p1}	1.2101
		k_{p2}	6.0726
		k_{i1}	0.4602
		k_{i2}	9.6519
		k_{d1}	0.4108
		k_{d2}	1.2732

TABLE IX: PERFORMANCE INDICES - CASE 2

Controller	Performance Index	ITAE		
		ΔF_1	ΔF_2	$\Delta P_{tie12,err}$
I	Settling time(s)	12	11	13
	Undershoot(Hz)	0.148	0.134	0.0025
	Overshoot(Hz)	0.063	0.065	0.0125
PI	Settling time(s)	12	10	13
	Undershoot(Hz)	0.16	0.145	0.0001
	Overshoot(Hz)	0.045	0.05	0.0125
PID	Settling time(s)	**3**	**5**	**3**
	Undershoot(Hz)	0.073	0.028	0.0125
	Overshoot(Hz)	0.0015	0.0207	0.001

B. Quantitative and Qualitative Analysis: Case 2

With reference to the analysis done for Case 1, it is evident that ITAE gives acceptable results. Hence with ITAE the simulation for bilateral contracts with violation is run. The best cost obtained using PID-ITAE is 0.01150, as shown in Table VIII. The ITAE obtained using PID is improved by 96% compared to ITAE-PI and ITAE-I. The gains of I, PI and PID controllers optimized with ITAE are given in Table VIII for violation of contracts. Overshoot (OS), undershoot (US) and settling time (ST) of deviations in frequencies and tie-line power transfer are given in Table IX.

From the initial portion of the curves in Fig. 7 and Fig. 8, it can be observed that undershoot; peak overshoot and the settling time are considerably less with PID controller compared between I and PI. The damping is poor for IAE-PID. The tie-line power deviation is a smooth curve without much fluctuation for PID as seen from Fig. 9. The scheduled tie-line power flow of 0.0125 pu MW is reached with PID in a short span of time without much oscillations. The performance indices for Case 2 are presented in the below Table IX.

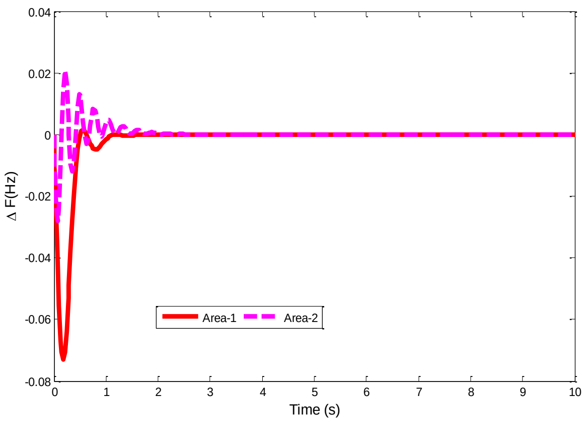

Fig. 7. Frequency deviations in Area-1 and Area-2 - Case 2.

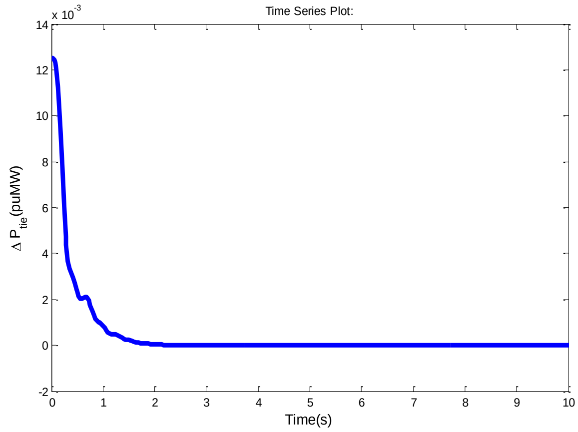

Fig. 8. Tie-line power deviation between Area-1 and Area-2 - Case 2.

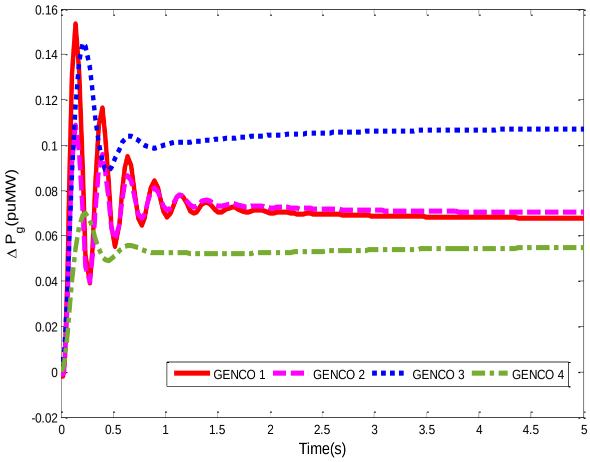

Fig. 9. Generation response of the GCs in Area-1&2 - Case 2.

As seen from the Table IX, PID with ITAE outperforms the other combinations. From the generation response curves, it is clear that the IAE–I and IAE-PI show increased overshoots and undershoots. IAE-PID has poor damping. The initial portion of the curve of PID shows more fluctuations whereas the overshoot is comparatively less. Hence ISE is selected for further investigation. The output responses obtained for Case 2 are shown in Fig. 7 to Fig. 9.

C. Robustness Analysis

To prove the robustness of the controller with ITAE as the objective function for optimization, the load perturbation of 20% and 30% are applied and the results are compared with that the base case (10% load perturbation). The optimized gains of the PID controller obtained using ITAE index are preserved and used for simulation for robustness analysis. The load changes are applied in both areas. The scheduled tie-line power and the change in the outputs of the GCs are tabulated in Table X.

TABLE X. ROBUSTNESS ANALYSIS

Load perturbation	ΔP_{tieach}	ΔP_{g1ss}	ΔP_{g2ss}	ΔP_{g3ss}	ΔP_{g4ss}
	(p.u. MW)				
10%	-0.0125	0.0375	0.05	0.0725	0.04
20%	-0.025	0.075	0.1	0.145	0.08
30%	-0.0375	0.1125	0.15	0.2175	0.12

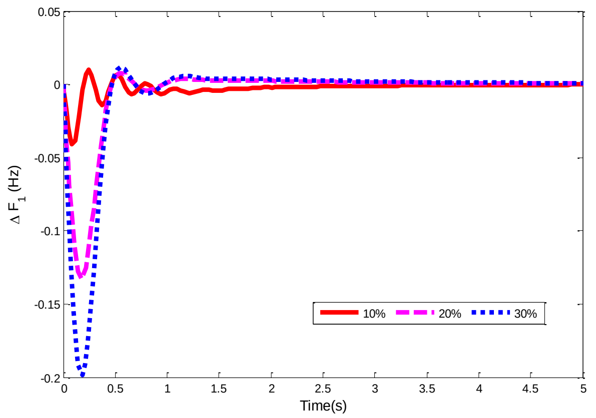

Fig. 10. Frequency deviation in Area-1 for different load perturbations.

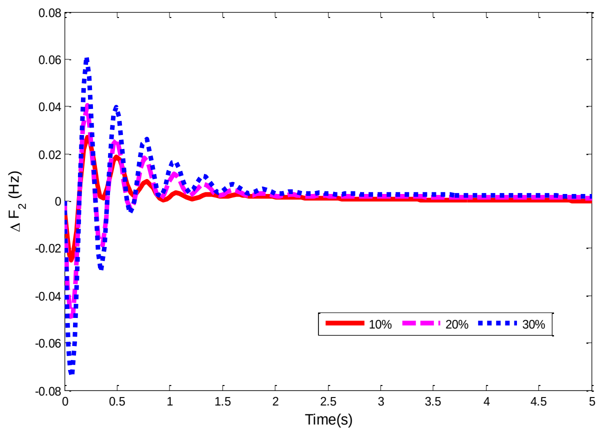

Fig. 11. Frequency deviation in Area-2 for different load perturbations.

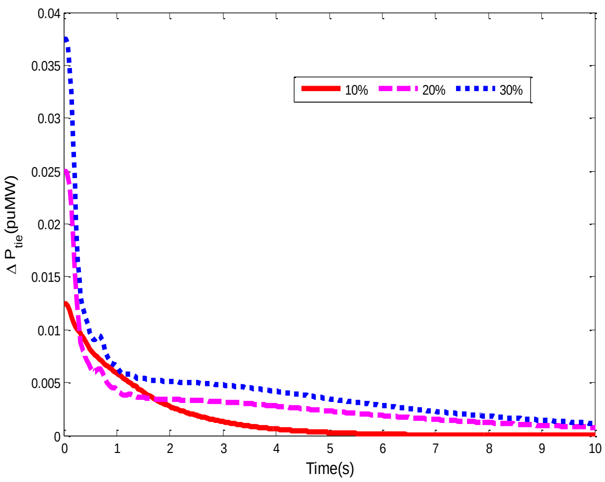

Fig. 12. Tie-line power deviation for different load perturbations.

The simulated frequency deviations, tie-line power deviations and generation responses of the four GCs in Area-1 and Area-2 are shown in Fig. 10, Fig. 11 and Fig. 12. The results validate the satisfactory performance of the optimal controller-objective function combination.

VII. CONCLUSIONS

In this paper, AGC under bilateral contract scenario with and without contract violation are analyzed. The gains of the controllers I, PI and PID are estimated with three different error criterions IAE, ISE, and ITAE. Using these controller gains, the scheduled tie-line power flows and the responses of the GCs in the two identical areas are calculated. The results show that ITAE with PID gives better results in terms of fast damping, reduced overshoot and undershoots. The settling time also reduced for the above combination indicating that the system reaches the steady state quickly within a short span of time. The robustness of the optimal combination is verified for 20% and 30% load perturbations, by retaining the optimized gains. The simulation results show that the PID controller- ITAE combination is able to alleviate the deviations in frequencies and tie-line power exchange in an ancillary market structure.

REFERENCES

[1] H. Glavitsch and J. Stoffel, "Automatic generation control," *Int. Journal of Electrical Power & Energy Systems*, vol. 2, no. 1, pp. 21-28, 1980.

[2] N. Jaleeli, L. S. VanSlyck, D. N. Ewart, L. H. Fink, and A. G. Hoffmann, "Understanding automatic generation control," *IEEE Trans. on Power Systems*, vol. 7, no. 3, pp. 1106-1122, Aug. 1992.

[3] R. D. Christie and A. Bose, "Load frequency control issues in power system operations after deregulation," *IEEE Trans. on Power Systems*, vol. 11, no. 3, pp. 1191-1200, Aug. 1996

[4] R. K. Green, "Transformed automatic generation control," *IEEE Trans. Power Syst.*, vol. 11, no. 4, pp. 1799-1804, Nov. 1996.

[5] B. H. Bakken and O. S. Grande, "Automatic generation control in a deregulated power system," *IEEE Trans. on Power Systems*, vol. 13, no. 4, pp. 1401-1406, Nov. 1998.

[6] Ibraheem, P. Kumar, and D. P. Kothari, "Recent philosophies of automatic generation control strategies in power systems," *IEEE Trans. on Power Systems*, vol. 20, no. 1, pp. 346-357, Feb. 2005.

[7] V. Donde, M. A. Pai, and I. A. Hiskens, "Simulation and optimization in an AGC system after deregulation," *IEEE Power Engineering Review*, vol. 21, no. 8, pp. 58-58, Aug. 2001.

[8] P. Dash, L. C. Saikia, and N. Sinha, "Comparison of performances of several Cuckoo search algorithms based 2DOF controllers in AGC of multi-area thermal system," *Int. Journal of Electrical Power & Energy Systems*, vol. 55, pp. 429-436, Feb. 2014.

[9] A. Khodabakhshian and R. Hooshmand, "A new PID controller design for automatic generation control of hydropower systems," *Int. Journal of Electrical Power & Energy Systems*, vol. 32, no. 5, pp. 375-382, 2010,

[10] B. K. Sahu, T. K. Pati, J. R. Nayak, S. Panda, and S. K. Kar, "A novel hybrid LUS–TLBO optimized fuzzy-PID controller for load frequency control of multi-source power system," *Int. Journal of Electrical Power & Energy Systems*, vol. 74, pp. 58-69, Jan. 2015.

[11] J. R. Nayak, B. Shaw, and B. K. Sahu, "Application of adaptive-SOS (ASOS) algorithm-based interval type-2 fuzzy-PID controller with derivative filter for automatic generation control of an interconnected power system," *Engineering Science and Technology, an International Journal*, vol. 21, no. 3, pp. 465-485, 2018.

[12] A. R. Joseph and A. Thomas, "A genetic proportional integral derivative controlled hydrothermal automatic generation control with superconducting magnetic energy storage," in *Electricity Distribution*, Panagiotis Karampelas and Lambros Ekonomou Ed. Springer Berlin Heidelberg, 2016, pp. 267-284.

[13] R. S. Kumar and R. Shivakumar, "Ant lion optimization approach for load frequency control of multi-area interconnected power systems," *Circuits and Systems*, vol. 7, no. 9, pp. 2357-2383, 2016.

[14] L. C. Saikia, J. Nandaand, and S. Mishra, "Performance comparison of several classical controllers in AGC for the multi-area interconnected thermal system," *Int. Journal of Electric Power Energy Systems*, vol. 33, no. 3, pp. 394–401, 2011.

[15] D. Puja, L. C. Saikia, and N. Sinha, "Flower pollination algorithm optimized PI-PD cascade controller in automatic generation

control of a multi-area power system," *Int. Journal of Electrical Power & Energy Systems*, vol. 82, pp. 19-28, Nov. 2016.

[16] R. More, L. C. Saikia, and N. Sinha, "Automatic generation control of a multi-area system using ant lion optimizer algorithm based PID plus second order derivative controller," *Int. Journal of Electrical Power & Energy Systems*, vol. 80, pp. 52-63, Sep. 2016.

[17] Y. Arya and N. Kumar, "Design and analysis of BFOA-optimized fuzzy PI/PID controller for AGC of multi-area traditional/restructured electrical power systems," *Soft Computing*, vol. 21, no. 21, pp. 6435-6452, 2017.

[18] H. M. Hasanien, "Whale optimization algorithm for automatic generation control of interconnected modern power systems including renewable energy sources," *IET Generation, Transmission & Distribution*, vol. 12, no. 3, pp. 607-614, 2017.

[19] A. Singh, N. Kumar, B. P. Joshi, and K. S. Vaisla, "AGC using adaptive optimal control approach in restructured power system," *Journal of Intelligent & Fuzzy Systems*, vol. 35, no. 5, pp. 4953-4962, 2018.

[20] J. Morsali, K. Zare, and M. T. Hagh, "A novel dynamic model and control approach for SSSC to contribute effectively in AGC of a deregulated power system," *Int. Journal of Electrical Power & Energy Systems*, vol. 95, pp. 239-253, Feb. 2018.

[21] P. C. Sahu, R. C. Prusty, and S. Panda, "Approaching hybridized GWO-SCA based type-II fuzzy controller in AGC of diverse energy source multi area power system," *Journal of King Saud University-Engineering Sciences*, 2019.

[22] T. S. Gorripotu, H. Samalla, C. J. M. Rao, A. T. Azar, and D. Pelusi, "TLBO algorithm optimized fractional-order PID controller for AGC of interconnected power system," in *Proc. Soft Computing in Data Analytics*, Springer, Singapore, 2019, pp. 847-855.

[23] K. Simhadri, B. Mohanty, and U. M. Rao, "Optimized 2DOF PID for AGC of multi-area power system using dragonfly algorithm," in *Applications of Artificial Intelligence Techniques in Engineering*, H. Malik, S. Srivastava, Y. R. Sood and A. Ahmad, Ed. Singapore: Springer, 2019, pp. 11-22.

[24] S. Mirjalili, "The ant lion optimizer," *Advances in Engineering Software*, pp. 80-98, 2015.

S. Jennathu Beevi received the B.E. degree from the Department of Electrical and Electronics Engineering, University of Madras, India, 1998. She obtained her M.E degree in power system engineering from B.S.A. Crescent Engineering College. She was awarded the silver medal for securing the second rank in M.E. Power System by Anna University in the year 2004. She is working as assistant professor (Senior Grade) in the Department of Electrical and Electronics Engineering, B.S. Abdur Rahman Institute of Science and Technology, Chennai. She is currently pursuing her Ph.D. at B.S. Abdur RahmanInstitute of Science and Technology in the area of automatic generation control in deregulated environment. She has been teaching for the past 16 years. Her research interests are in the field of optimization in deregulated power system, power system control and soft computing.

Dr. R. Jayashree secured her B.E degree in electrical and electronics engineering in the year 1990 with a first class from Thiagarajar College of Engineering, Madurai. She secured her M.E. degree in power system engineering with first class with distinction at Anna University, Chennai in the year 1992. She secured first rank in M.E. degree. She secured her Ph.D. degree in electrical engineering at Anna University, Chennai in the year 2008. She is currently working as Professor at B.S. Abdur Rahman Institute of Science and Technology. She has been teaching for the past 23 years. She is a member of IEEE. She has to her credit about 55 papers published/presented in the National and International journals/conferences. Her areas of interest include ATC and congestion management, load frequency control, reactive power allocation and pricing etc.